53BP1 loss rescues BRCA1 deficiency and is associated with triple-negative and BRCA-mutated breast cancers

Peter Bouwman[1,10], Amal Aly[2,10], Jose M Escandell[3,10], Mark Pieterse[1], Jirina Bartkova[4], Hanneke van der Gulden[1], Sanne Hiddingh[1], Maria Thanasoula[3], Atul Kulkarni[2], Qifeng Yang[2], Bruce G Haffty[2], Johanna Tommiska[5], Carl Blomqvist[6], Ronny Drapkin[7], David J Adams[8], Heli Nevanlinna[5], Jiri Bartek[4,9], Madalena Tarsounas[3], Shridar Ganesan[2] & Jos Jonkers[1]

Germ-line mutations in *breast cancer 1, early onset* (*BRCA1*) result in predisposition to breast and ovarian cancer. *BRCA1*-mutated tumors show genomic instability, mainly as a consequence of impaired recombinatorial DNA repair. Here we identify p53-binding protein 1 (53BP1) as an essential factor for sustaining the growth arrest induced by *Brca1* deletion. Depletion of 53BP1 abrogates the ATM-dependent checkpoint response and G2 cell-cycle arrest triggered by the accumulation of DNA breaks in *Brca1*-deleted cells. This effect of 53BP1 is specific to BRCA1 function, as 53BP1 depletion did not alleviate proliferation arrest or checkpoint responses in *Brca2*-deleted cells. Notably, loss of 53BP1 partially restores the homologous-recombination defect of *Brca1*-deleted cells and reverts their hypersensitivity to DNA-damaging agents. We find reduced 53BP1 expression in subsets of sporadic triple-negative and BRCA-associated breast cancers, indicating the potential clinical implications of our findings.

BRCA1 and BRCA2 are large phosphoproteins involved in DNA-damage repair through homologous recombination (HR)[1]. Although BRCA1 and BRCA2 share many interacting proteins, they show little homology and are thought to have different roles in HR and other processes[2]. BRCA1 is thought to be mainly a scaffold protein enabling interactions between different components of the HR machinery, whereas BRCA2 is directly involved in loading RAD51 to sites of damage or stalled replication forks[3].

Heterozygous *BRCA1* and *BRCA2* inactivation mutations are associated with an increased risk to develop breast and ovarian cancers. These tumors often show loss of heterozygosity of the wild-type allele and mutation of the p53 tumor suppressor[4,5]. Breast cancers that arise in *BRCA1* mutation carriers are mostly high-grade tumors with the so-called triple-negative phenotype (that is, lacking expression of estrogen receptor and progesterone receptor and without amplification of human epidermal growth factor receptor (ERBB2/HER2))[6]. BRCA1-associated tumors also express basal epithelial cell markers, such as cytokeratin 5/6 (ref. 7), and cluster with basal-like breast cancers by gene expression profiling[8]. There is increasing evidence that a subset of sporadic tumors with a basal-like/triple-negative phenotype may have alterations in BRCA1-related pathways[9]. In contrast, *BRCA2* mutation carriers develop mostly ER-positive breast cancers.
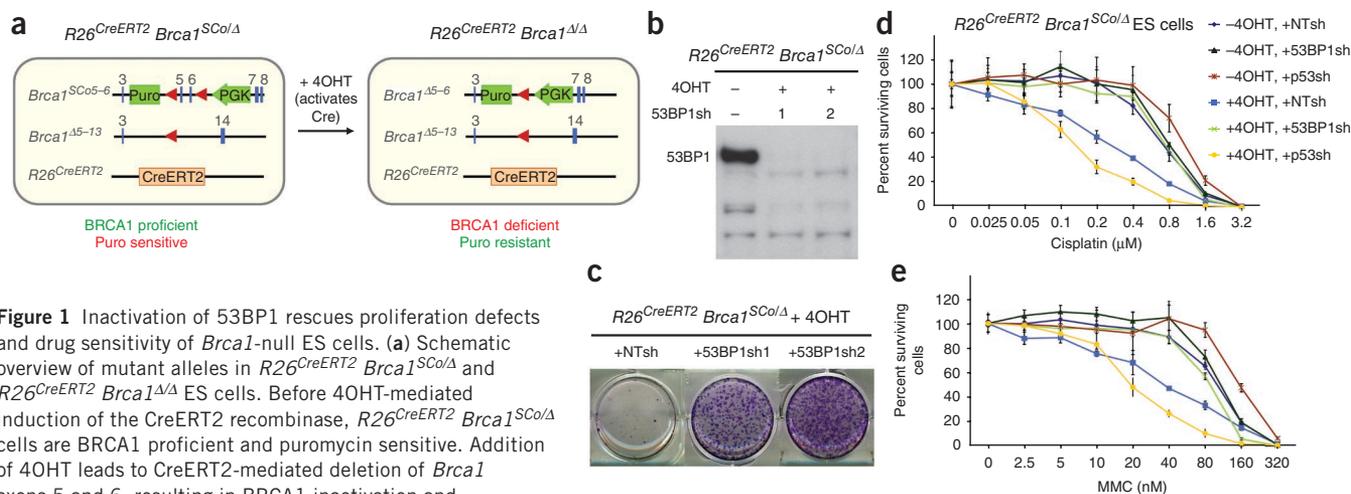
Whereas BRCA1 and BRCA2 function as tumor suppressors in breast and ovarian epithelium, homozygous deletion of BRCA1 or

BRCA2 appears not to be tolerated during human or mouse development and in cultured primary cells such as mouse embryonic fibroblasts (MEFs) or stem cells[10]. Although concomitant deletion of p53 partially alleviates these phenotypes[11], the incomplete rescue suggests the involvement of other factors in BRCA1/2 associated cancers. In search for such factors, using a candidate gene approach, knockout of 53BP1 was shown in a recent study[12] to rescue *Brca1* hypomorphic MEFs and mice from premature senescence. 53BP1, a DNA-damage response (DDR) factor involved in both HR and nonhomologous end joining (NHEJ), is known to be an activator of p53 (ref. 13). However, 53BP1 also has p53 independent functions, and deletion of both 53BP1 and p53 has a synergistic effect on tumor development[14,15].

The observations in the *Brca1* hypomorphic mutants raise some intriguing questions. First, will 53BP1 ablation also rescue cells completely deficient for BRCA1, a situation that is common in BRCA1-associated tumors? In contrast to *Brca1*-null mice, the *Brca1*[Δ11/Δ11] hypomorphic mice still express the natural BRCA1-Δ11 splice variant, which contains the conserved RING and BRCT domains[10]. The *Brca1*[Δ11] allele is functionally active, as evidenced by the fact that homozygous *Brca1*[Δ11/Δ11] mutants are viable on a p53 heterozygous background[16]. Other questions concern the mechanism by which deletion of 53BP1 rescues BRCA1-deficient cells and the potential relevance of 53BP1 status for BRCA1-associated cancers.

Figure 1 Inactivation of 53BP1 rescues proliferation defects and drug sensitivity of *Brca1*-null ES cells. (**a**) Schematic overview of mutant alleles in *R26^CreERT2 Brca1^SCo/Δ* and *R26^CreERT2 Brca1^Δ/Δ* ES cells. Before 4OHT-mediated induction of the CreERT2 recombinase, *R26^CreERT2 Brca1^SCo/Δ* cells are BRCA1 proficient and puromycin sensitive. Addition of 4OHT leads to CreERT2-mediated deletion of *Brca1* exons 5 and 6, resulting in BRCA1 inactivation and concomitant expression of puromycin from the PGK promoter, thereby enabling selection of BRCA1-deficient *R26^CreERT2 Brca1^Δ/Δ* ES cells. (**b**) Western blot analysis of 53BP1 expression in *R26^CreERT2 Brca1^SCo/Δ* ES cells nontransduced or transduced with two independent lentiviral shRNA vectors against *53bp1*, after treatment with 4OHT to delete the *Brca1^SCo* allele. (**c**) Crystal violet staining of nontransduced *R26^CreERT2 Brca1^SCo/Δ* ES cells treated with 4OHT and stably transduced with lentiviral vectors expressing a control nontargeting shRNA (NT) or two independent shRNAs against *53bp1*. (**d,e**) Susceptibility of *R26^CreERT2 Brca1^SCo/Δ* ES cells untreated or treated with 4OHT to DNA cross-linking agents cisplatin (**d**) or mitomycin C (**e**). Cell viability was measured after 4 d. Mean ± s.d. is shown from three independent measurements.

In this work, we set out to explore these questions. We performed an unbiased transposon mutagenesis screen for factors that could restore normal growth of *Brca1*-null cells. Similar to the observations with *Brca1^Δ11* hypomorphic mutants, clonal outgrowth of *Brca1*-null cells was rescued by a loss of function mutation of 53BP1. We show that cells lacking both BRCA1 and 53BP1 have a partially restored HR pathway. The clinical relevance of these findings is indicated by our data showing that 53BP1 expression is reduced in a subset of basal-like/triple-negative breast cancers and in BRCA1/2-associated breast cancers, suggesting positive selection for loss of 53BP1 function in these tumors.

RESULTS

53BP1 loss rescues proliferation defects of *Brca1*-null cells

Brca1 deletion in p53-proficient normal cells leads to a severe proliferation defect[17]. Cre/loxP-based conditional *Brca1* knockout models would not be useful to screen for factors that enhance growth of BRCA1-deficient cells, as *Brca1*-deleted cells are rapidly eliminated and the culture is rapidly overtaken by BRCA1-proficient cells. To overcome this problem, we generated *R26^CreERT2 Brca1^SCo/Δ* mouse embryonic stem (ES) cells, which contain, in addition to a *Brca1^Δ5−13*-null allele[18], a *Brca1* selectable conditional (*Brca1^SCo*) knockout allele in which exons 5 and 6 are flanked by loxP recombination sites and a split puromycin resistance marker (**Fig. 1a** and **Supplementary Fig. 1a**). Furthermore, these cells contain the *CreERT2* gene targeted to the *Rosa26* locus, leading to expression of a tamoxifen-inducible CreERT2 recombinase fusion protein[19]. Incubation of these cells with 4-hydroxytamoxifen (4OHT) resulted in nearly complete switching of the *Brca1^SCo* allele and consequent loss of BRCA1 protein expression (**Supplementary Fig. 1b,c**). Nonswitched *R26^CreERT2 Brca1^SCo/Δ* cells were effectively removed by puromycin selection (**Supplementary Fig. 1e**).

We used the piggyBac transposon system[20] to perform an insertional mutagenesis screen for factors that rescue the proliferation defect of *Brca1*-deleted cells (**Supplementary Data**). We transfected *R26^CreERT2 Brca1^SCo/Δ* ES cells with plasmids containing an engineered piggyBac transposon and mouse codon–optimized piggyBac transposase. After
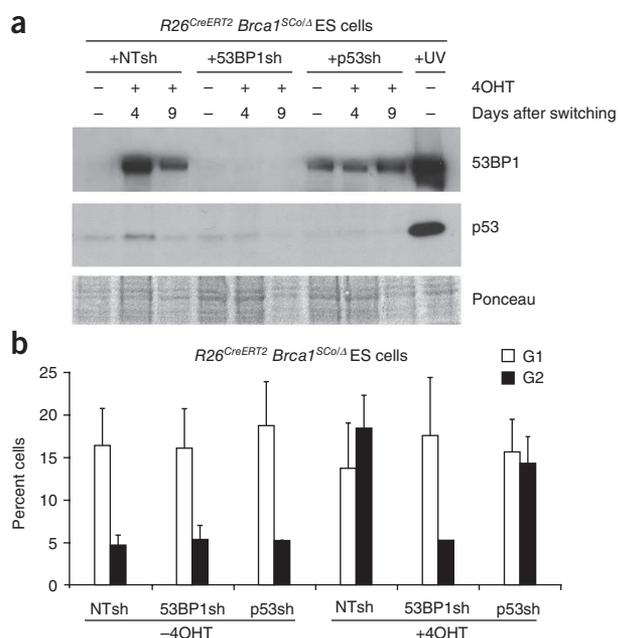
induction of CreERT2-mediated deletion of the *Brca1^SCo* allele with 4OHT, we assayed for clonal survival of BRCA1-deficient ES cells under puromycin selection (**Supplementary Fig. 2a**). The majority (294 out of 296) of surviving colonies analyzed contained both a switched and a nonswitched *Brca1^SCo* allele, indicating strong selection for allele duplication events (data not shown). Two clones that were completely *Brca1* deleted showed identical patterns of piggyBac transposon integrations (**Supplementary Fig. 2b**), one of which mapped to intron 16 of the *53bp1* gene (**Supplementary Fig. 2c**) and correlated with abrogation of 53BP1 expression (**Supplementary Fig. 2d**), consistent with the reported ability of 53BP1 deletion to abrogate senescence and cell death in *Brca1^Δ11/Δ11* hypomorphic cells[12]. To validate the loss of 53BP1 expression as a survival factor in *Brca1*-null cells, we tested the effects of shRNA-mediated depletion of 53BP1 in *R26^CreERT2 Brca1^SCo/Δ* ES cells with two different shRNAs that efficiently suppressed 53BP1 expression, as determined by western blot analysis (**Fig. 1b**). The robust clonal growth arrest of *R26^CreERT2 Brca1^SCo/Δ* ES cells induced by 4OHT treatment was abolished when 53BP1 was depleted with either shRNA (**Fig. 1c**).

53BP1 loss rescues drug hypersensitivity of *Brca1*-null cells

A hallmark of BRCA1-deficient tumors is their cisplatin sensitivity[21]. Consistent with this, we observed enhanced cytotoxicity of cisplatin in our *Brca1*-deleted ES cells (**Fig. 1d**). shRNA-mediated loss of 53BP1 fully abolished the cisplatin sensitivity induced by *Brca1* inactivation (**Fig. 1d**). We observed a similar reversal of drug sensitivity by 53BP1 depletion for mitomycin C (**Fig. 1e**). Although shRNA-mediated inhibition of p53 suppressed the growth defects of *Brca1*-deleted cells (data not shown), it did not suppress cisplatin sensitivity, suggesting that p53 and 53BP1 provide distinct pathways for sustaining growth arrest in *Brca1*-deleted cells.

53BP1 loss blocks DNA-damage responses in *Brca1*-null cells

To investigate how suppression of 53BP1 or p53 alleviates the impaired proliferation of *Brca1*-knockout ES cells, we analyzed cell-cycle profiles of 4OHT-treated *R26^CreERT2 Brca1^SCo/Δ* cells treated with control shRNA or shRNA causing depletion of 53BP1 or p53,

Figure 2 53BP1 depletion rescues cell-cycle defects of *Brca1*-null ES cells. (**a**) Western blot analysis of 53BP1 and p53 expression in *R26^{CreERT2} Brca1^{SCo/Δ}* ES cells stably tranduced with lentiviral shRNA vectors against *53bp1* or *p53*. Samples were taken before or at 4 and 9 d after 4OHT-induced deletion of *Brca1*. (**b**) Flow cytometry profiles of *R26^{CreERT2} Brca1^{SCo/Δ}* ES cells stably transduced with nontargeting shRNA lentiviruses or shRNA vectors against *53bp1* and *p53*. Shown are percentages of cells in G1 and G2 before or 9 d after 4OHT-induced *Brca1* deletion by CreERT2. Mean ± s.d. is shown from two experiments.

Brca1 gene, we observed robust phosphorylation of the DNA-damage checkpoint kinase CHK2 as well as p53 accumulation, indicative of an ATM-dependent DDR in MEFs (**Fig. 3a**, +Cre, GFPsh). Similar to the G2 arrest, this ATM-dependent checkpoint response was markedly attenuated upon 53BP1 inhibition (**Fig. 3a**, +Cre, 53BP1sh1 and 53BP1sh2).

Consistent with unrepaired DNA damage being the cause of the observed G2/M arrest and checkpoint activation triggered by *Brca1* deletion, we observed a marked increase in chromatid and chromosome breaks in BRCA1-deficient MEFs (**Fig. 3b**). shRNA-mediated 53BP1 depletion in these cells led to a decrease in the occurrence of DNA breaks, reflected in diminished checkpoint responses.

In contrast to *Brca1*-knockout MEFs, proliferation of *Brca2*-knockout MEFs[25] was not rescued by shRNA-mediated depletion of 53BP1 (**Fig. 3c**). In contrast, p53 inhibition efficiently restored the proliferative capacity of *Brca2*-deleted cells. Consistent with the role of 53BP1 in mediating checkpoint responses specifically in cells lacking *Brca1*, 53BP1 abrogation did not affect CHK2 phosphorylation in BRCA2-deficient MEFs (**Fig. 3d**). This observation reflects the fundamentally distinct roles played by the BRCA1 and BRCA2 tumor-suppressor proteins in the DDR: whereas BRCA1 is required for the initial steps of the DDR response and signal amplification, BRCA2 functions downstream of the checkpoint signaling, promoting the HR pathway of DNA repair. Because 53BP1 acts during the early chromatin-remodeling events at the break, it is more likely to

monitored by western blotting (**Fig. 2a**). In the absence of BRCA1, ES cells accumulate in G2 (**Fig. 2b**), which could reflect a checkpoint response induced by accumulation of unrepaired DNA damage. This G2 arrest is abrogated in 53BP1-deleted cells but not in p53-depleted cells, suggestive of an ataxia-telangiectasia mutated (ATM)-dependent checkpoint activation for which 53BP1 is essential. Consistent with this, we observed an increase in 53BP1 expression levels in *Brca1*-deleted cells (**Fig. 2a**). The less pronounced effect of p53 depletion on the G2 arrest is mirrored by the lower induction of p53 expression in response to *Brca1* deletion, as detected by western blotting. p53 has a major role in the surveillance of chromosome integrity at the G1/S transition, although evidence for a relatively weaker p53-dependent checkpoint at the G2/M transition has also been reported[22,23].

To address the possibility that the loss of 53BP1 affects the DNA damage response (DDR) induced by *Brca1* deletion, we used MEFs that were established from mice carrying a *Brca1^{SCo}* allele and a *Brca1^{Δ5−13}*-null allele and immortalized by TBX2 overexpression. Transient expression of Cre recombinase from a self-deleting 'hit-and-run' (H&R) Cre retrovirus[24] resulted in efficient deletion of *Brca1* exons 5 and 6 and loss of BRCA1 expression, as monitored by western blotting (**Fig. 3a**). We detected concomitant loss of 53BP1 expression when MEFs were co-transduced with the H&R Cre and 53BP1 shRNA-encoding viruses. Upon Cre-mediated deletion of the
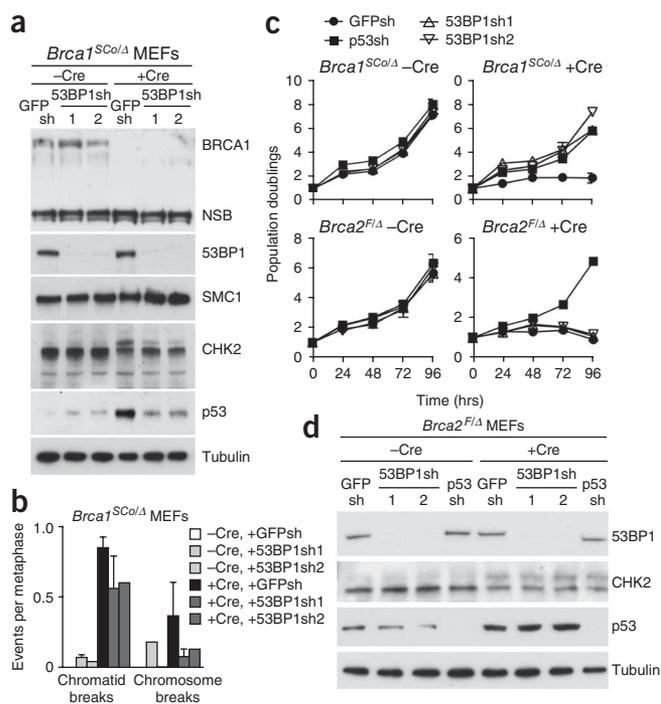
Figure 3 53BP1 depletion abrogates CHK2-mediated DNA-damage responses and rescues proliferation defects in *Brca1*-null but not *Brca2*-null MEFs. (**a**) Western blot analysis of cell extracts from *Brca1^{SCo/Δ}* MEFs infected with retroviruses expressing self-deleting Cre recombinase (+Cre) or empty vector (−Cre) together with retroviruses expressing 53BP1 or GFP control shRNAs. SMC1 and tubulin were used as loading controls. NSB, nonspecific band. (**b**) Quantification of chromatid and chromosome break frequency in metaphase spreads prepared from cells treated as in **a**. At least 100 metaphases were scored for each sample. Shown is the average number of events per metaphase ± s.d. (**c**) Proliferation curves of *Brca1^{SCo/Δ}* or *Brca2^{F/Δ}* MEFs infected with retroviruses expressing self-deleting Cre recombinase (+Cre) or empty vector (−Cre) together with retroviruses expressing p53, 53BP1 or GFP control shRNAs. (**d**) Western blot analysis of cell extracts from *Brca2^{F/Δ}* MEFs treated as in **c**. Tubulin was used as a loading control.

Figure 4 53BP1 depletion rescues RAD51 foci in *Brca1*-null cells. (**a**) RAD51 focus formation in *R26^CreERT2 Brca1^SCo/Δ* ES cells untreated or treated with 4OHT and transduced with lentiviruses expressing nontargeting shRNAs (NTsh) or shRNAs targeting *53bp1* (53BP1sh). Cells were irradiated with 10 Gy, fixed after 6 h and stained with anti-RAD51 antibody (red). Nuclei were visualized with 4′,6-diamidino-2-phenylindole (DAPI) (blue). (**b**) RAD51 focus formation in *Brca1^SCo/Δ* MEFs infected with retroviruses expressing self-deleting Cre recombinase (+Cre) or empty vector (−Cre) together with retroviruses expressing 53BP1 or GFP control shRNAs. Cells were irradiated with 10 Gy, fixed after 2 h and stained with anti-γH2AX (red) and anti-RAD51 antibodies (green). Nuclei were visualized with DAPI (blue). (**c**) Quantification of RAD51 foci in *R26^CreERT2;Brca1^SCo/Δ* ES cells treated as in **a**. At least 20 nuclei were analyzed for each treatment. (**d**) Quantification of RAD51 foci in *Brca1^SCo/Δ* MEFs treated as in **b**. At least 50 nuclei were analyzed for each treatment.

affect BRCA1-dependent signaling. In contrast, BRCA2 activation requires the damage signal generated at the break to be transduced downstream through at least two parallel pathways involving several response factors[26]. Thus, the loss of 53BP1 can be compensated by other regulatory mechanisms acting between the early events at the chromatin surrounding the break and the initiation of repair reactions. Although shRNA-mediated depletion of p53 rescues the proliferation defect of BRCA2-deficient cells, DDR activation shown by CHK2 phosphorylation persists. This suggests that CHK2-mediated p53 activation contributes to the senescence response induced by the loss of BRCA2. Consistent with the role of BRCA2 as the loader of RAD51 onto double-strand breaks (DSBs), the initiating step of recombinational DNA repair, we did not detect any rescue of RAD51 foci in BRCA2-deficient cells when either p53 or 53BP1 were depleted (data not shown).

Together, these results suggest that 53BP1 is required for efficient ATM-dependent checkpoint signaling to arrest cell-cycle progression in response to DNA damage accumulation in *Brca1*-deleted cells. Alternatively, 53BP1 loss might lead to more efficient DNA DSB repair and thereby reduce DDR activation.

53BP1 loss partially restores HR in *Brca1*-null cells

The observed abrogation of G2 accumulation, sensitivity to DNA cross-linkers and DDR may be due to a stimulation of BRCA1-independent DNA repair. Alternatively, checkpoint release might prevent the formation of DNA breaks by collapsing replication forks or allow the cells to continue cycling without actual repair of the damage. To investigate the effects of 53BP1 depletion on DNA repair, we analyzed RAD51 focus formation in *Brca1^SCo/Δ* and *Brca1^Δ/Δ* ES cells following treatment with ionizing irradiation (**Fig. 4**). Analysis of these ionizing

Table 1 Gene-targeting frequencies in *R26^CreERT2 Brca1^SCo/Δ* ES cells

			G418-resistant colonies		
	4OHT[a]	shRNA	Total analyzed	Nontargeted (%)	Targeted (%)
Rb	−	NT	78	70 (90)	8 (10)
	+	NT	78	78 (100)	0 (0)
	+	53BP1	160	158 (99)	2 (1)
	+	p53	124	124 (100)	0 (0)
Pim1	−	NT	56	47 (84)	9 (16)
	+	NT	11	11 (100)	0 (0)
	+	53BP1	47	43 (91.5)	4 (8.5)

[a]4-hydroxytamoxifen (4OHT) was added to induce deletion of *Brca1^SCo*.
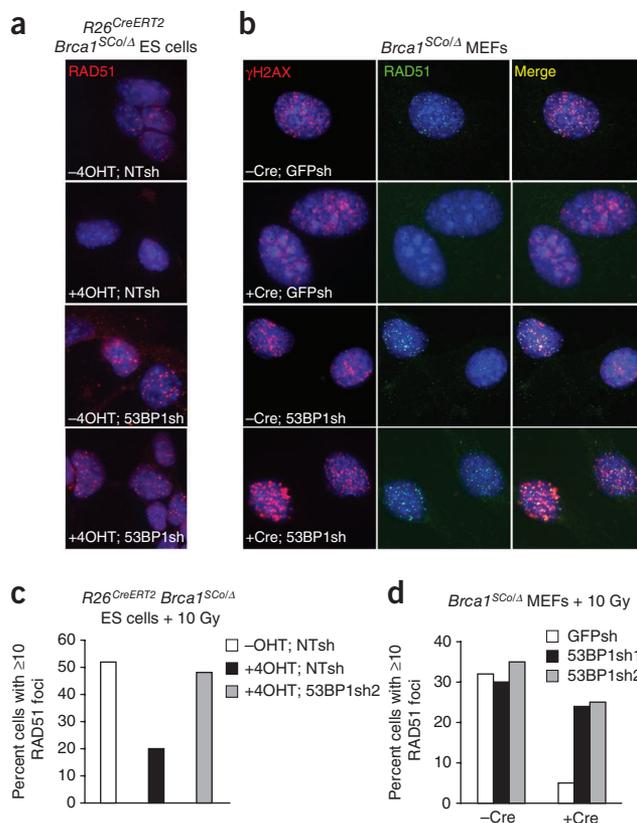
radiation–induced RAD51 foci revealed a diminished response upon deletion of *Brca1* (**Fig. 4a,c**), consistent with previous observations[27]. shRNA-mediated depletion of 53BP1 enhanced RAD51 focus formation in the absence of BRCA1, suggesting upregulation of HR in a BRCA1-independent manner. This process is not specific for ES cells, as we observed the same phenomenon in MEFs (**Fig. 4b,d**).

To determine whether 53BP1 depletion rescues homology-directed repair (HDR) in BRCA1-deficient cells, we measured gene-targeting efficiencies in *R26^CreERT2 Brca1^SCo/Δ* ES cells with or without shRNA-mediated depletion of 53BP1 or p53 using an isogenic *Rb*-targeting construct with a PGK-neo selection marker[28]. Whereas CreERT2-mediated deletion of *Brca1* by addition of 4OHT abolished *Rb* gene targeting in *R26^CreERT2 Brca1^SCo/Δ* ES cells, this effect could not be reversed by shRNA-mediated depletion of p53 (**Table 1**). In contrast, we observed correct integration of the targeting vector at the *Rb* locus in 2 out of 160 53BP1-depleted *R26^CreERT2 Brca1^Δ/Δ* ES cell colonies compared to 8 out of 78 *R26^CreERT2 Brca1^SCo/Δ* colonies, suggesting that 53BP1 loss leads to partial restoration of HDR in *Brca1*-null cells. This notion was supported by gene-targeting experiments with a promoterless *Pim1-neo* targeting construct[29], showing correct integration in 4 out of 47 53BP1-depleted *R26^CreERT2 Brca1^Δ/Δ* ES colonies compared to 9 out of 56 *R26^CreERT2 Brca1^SCo/Δ* colonies (**Table 1**). We conclude that depletion of 53BP1 restores HR activity in *Brca1*-null cells to 10–50% of that of BRCA1-proficient cells.

Basal-like breast cancers have low levels of 53BP1

The majority of BRCA1-associated tumors carry p53 mutations[30,31]. It is known that p53 loss can at least partially rescue BRCA1-deficient cells[11,32]. However, there may still be additional selection for aberrant expression of 53BP1, as suggested by our *in vitro* results and by the synergism in tumorigenesis observed in *53bp1^−/−^p53^−/−* knockout mice[14,15]. Therefore, we analyzed levels of *53BP1* mRNA in a publicly
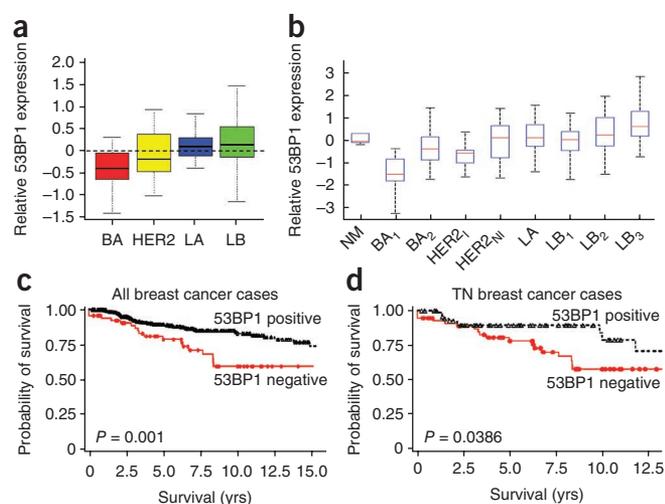
Figure 5 53BP1 expression is reduced in a subset of human BLC. (**a**) Boxplots showing 53BP1 expression levels among breast cancer subtypes. Gene expression array data from 286 early-stage breast cancers[33] were clustered to classify tumors into basal (BA), HER2-positive (HER2), luminal A (LA) and luminal B (LB). The mean expression values of 53BP1 are shown for each subgroup. (**b**) Boxplots showing 53BP1 expression levels among different breast cancer subtypes defined by robust consensus clustering: normal (NM), basal (BA_1, BA_2), HER2-positive ($HER2_I$, $HER2_{NI}$), and luminal (LA, LB_1, LB_2, LB_3). The data are normalized, with mean expression of the combined data being set to 0. Expression of 53BP1 is significantly lower in the BA_1 subtype ($P < 0.0001$ versus normal; $P < 0.0002$ versus BA_2). (**c,d**) Distant relapse–free survival stratified by 53BP1 protein expression in all breast cancers (**c**) and in triple-negative (TN) breast cancers (**d**). Kaplan-Meyer survival curves are shown for breast cancers that scored positive for 53BP1 staining (black lines) and those that scored negative for 53BP1 staining (red lines).

available database of gene expression array data from 286 breast cancer specimens[33], all early stage (lymph-node negative) and treated with surgery and radiation therapy alone. We used previously described unsupervised clustering methods to identify basal-like breast cancers (BLCs), HER2-positive breast cancers and luminal A and luminal B subclasses of breast cancer[34]. BLC tumors are characterized clinically as high-grade, invasive breast cancers that lack expression of estrogen receptor, progesterone receptor and HER2 (triple-negative phenotype) and are associated with a younger age of onset. Luminal tumors are characterized by expression of the estrogen receptor (ER+), with luminal A tumors being mostly low-grade ER+ tumors and luminal B tumors being mostly high-grade ER+ tumors. We next calculated mean levels of 53BP1 expression for each breast cancer subtype (**Fig. 5a**). We found the lowest *53BP1* expression levels in the BLC subclass.

We have previously shown that a robust consensus clustering approach of breast cancer gene-expression data reveals two subclasses of BLC, which we labeled BA_1 and BA_2 (ref. 34). This approach also identifies two subclasses of HER2-positive cancers and three subclasses of luminal B tumors. We examined *53BP1* mRNA expression in these different subclasses in a combined dataset that includes the published datasets of two previous reports[33,35]. In this combined dataset, we found that *53BP1* expression was clearly lowest in the BA_1 subtype of BLC ($P < 0.0001$ versus normal, $P < 0.0002$ versus BA_2) (**Fig. 5b**). These data suggest that a biologically relevant subset of BLC has low *53BP1* expression. To validate this finding at the protein level, we assayed a set of 504 breast cancer specimens from the Yale cohort by immunohistochemistry on tissue microarrays. The clinical characteristics of the tumors in this collection are shown in **Supplementary Table 1**. Four hundred forty-four cases were evaluable for 53BP1 status. We scored a specimen as lacking 53BP1 staining if <10% of tumor cells showed nuclear staining with this antibody (**Supplementary Fig. 3**). Out of 444 evaluable breast cancer specimens, we scored 65 (14.6%) as being negative for 53BP1.

53BP1 loss is associated with triple-negative phenotype
In the Yale cohort of 444 tumors, lack of 53BP1 staining correlated independently with lack of estrogen receptor expression, lack of progesterone receptor expression and lack of HER2 overexpression, as assessed by immunohistochemistry (**Table 2**). There was a striking correlation between the absence of 53BP1 staining and the triple-negative phenotype, defined as being ER-, PR- and HER2-negative. Of the 63 tumors in the Yale cohort that lacked 53BP1 staining and

for which ER, PR and HER2 status were available, 57 (90.5%) of these tumors were triple-negative tumors. Of the 132 triple-negative tumors assayed, 57 (43%) were 53BP1 negative, whereas of the 311 non–triple-negative tumors, only 6 (2%) had reduced 53BP1 staining. This correlation was statistically significant ($P < 0.0001$). The immunohistochemistry data are consistent with the gene-expression data and confirm that a subset of BLCs and triple-negative tumors have a profoundly decreased 53BP1 expression. Loss of 53BP1 was associated with age below 50, with most (67%) of 53BP1-negative tumors occurring in women less than 50 years old. There was no correlation with tumor size, lymph-node status or race.

53BP1 loss is associated with *BRCA1/2* mutation status
To validate and extend the data from the Yale cohort, including assessment of 53BP1 protein expression in *BRCA1/2*-mutated familial breast carcinomas, we performed an independent larger-tissue microarray analysis on the Helsinki cohort of 1,187 patients (**Table 3**). We obtained these data using different 53BP1 antibodies, and the data were analyzed independently by separate pathologists (see **Supplementary Fig. 4** for examples of 53BP1 staining patterns in the Helsinki cohort). Confirming the results obtained from the Yale cohort, lack of 53BP1 staining in the Helsinki cohort correlated independently with lack of estrogen receptor expression ($P = 0.000004$), lack of progesterone receptor expression ($P = 0.003$) and the triple-negative phenotype

Table 2 Low 53BP1 expression correlates with triple-negative status (Yale cohort)

Features	53BP1 expression			P^a
	Total (%)	Positive (%)	Negative (%)	
Estrogen receptor				
Positive	243 (55)	239 (63)	4 (6)	
Negative	200 (45)	140 (37)	60 (94)	<0.0001
Progesterone receptor				
Positive	226 (51)	222 (59)	4 (6)	
Negative	217 (49)	157 (41)	60 (94)	<0.0001
ERBB2/HER2				
Positive	78 (18)	77 (20)	1 (2)	
Negative	366 (82)	303 (80)	63 (98)	<0.0001
Triple-negative (TN)				
Not TN	311 (70)	305 (80)	6 (10)	
TN	132 (30)	75 (20)	57 (90)	<0.0001

^{a}Fisher's exact test.

Table 3 Loss or reduction of 53BP1 expression correlates with triple-negative status and BRCA1/2 mutation status (Helsinki cohort)

Features	53BP1 Total (%)	Normal (%)	Aberrant (%)	P^a
Estrogen receptor	1,053			
Positive	834 (79.2)	823 (80.3)	11 (39.3)	
Negative	219 (20.8)	202 (19.7)	17 (60.7)	0.000004
Progesterone receptor	1,050			
Positive	703 (67.0)	692 (67.7)	11 (39.3)	
Negative	347 (33.0)	330 (32.3)	17 (60.7)	0.003
ERBB2/HER2	1,075			
Positive	145 (13.5)	142 (13.6)	3 (10.3)	
Negative	930 (86.5)	904 (86.4)	26 (89.7)	0.8
Triple-negative (TN)	1,018			
Not TN	875 (86.0)	861 (87.0)	14 (50.0)	
TN	143 (14.0)	129 (13.0)	14 (50.0)	0.000004
BRCA1/2 mutation	1,187			
Non-BRCA1/2	1,108 (93.4)	1,079 (94.0)	29 (74.4)	0.000003^b
Sporadic	374	371	3	0.001^c
Familial non-BRCA1/2	734	708	26	
BRCA1/2	79 (6.6)	69 (6.0)	10 (25.6)	0.0001^d
BRCA1	35	30	5	0.003^e
BRCA2	44	39	5	0.008^f

[a]Fisher's exact test. [b]BRCA1/2 versus sporadic. [c]BRCA1/2 versus familial non-BRCA1/2 tumors. [d]BRCA1/2 vs. all non-BRCA1/2 tumors (sporadic + familial non-BRCA1/2). [e]BRCA1 versus all non-BRCA1/2 tumors. [f]BRCA2 versus all non-BRCA1/2 tumors.

($P = 0.000004$). In addition, the familial tumors from *BRCA1/2* mutation carriers (79 tumors) showed the highest degree of aberrant 53BP1 reduction or loss compared to sporadic tumors ($n = 374$, $P = 0.000003$), familial carcinomas not attributable to *BRCA1/2* mutations ($n = 734$, $P = 0.001$) or all non-BRCA1/2 tumors ($n = 1,108$, $P = 0.0001$). Both BRCA1- and BRCA2-associated tumors showed a significantly increased incidence of reduced 53BBP1 staining compared to non-BRCA1/2 tumors ($P = 0.003$ for BRCA1 and $P = 0.008$ for BRCA2). Overall, these results show that loss of 53BP1 is more frequent among the most aggressive and difficult-to-treat triple-negative tumors as well as in tumors with *BRCA1/2* mutations.

53BP1 expression and distant metastasis–free survival

We analyzed the survival data from the Yale cohort. There was significant association between 53BP1 status and distant metastasis–free survival, with 53BP1-negative tumors having significantly lower metastasis-free survival (**Fig. 5c**) ($P = 0.001$). As most tumors that lack 53BP1 have a triple-negative phenotype, we analyzed distant metastasis–free survival in triple-negative breast cancers stratified by 53BP1 status. Amongst the triple-negative tumors, those that lack normal 53BP1 staining have decreased metastasis-free survival ($P = 0.039$) (**Fig. 5d**). As the cancers in this dataset were mostly early-stage, lymph node–negative cancers that did not receive any adjuvant treatment, these data suggest that early-stage triple-negative tumors with reduced 53BP1 may have a greater likelihood of metastasis in the absence of systemic treatment compared to triple-negative tumors with intact 53BP1.

DISCUSSION

BRCA1 is a large ubiquitously expressed protein that has a major role in DDR by HR. Its activity is extensively regulated by phosphorylation[36], sumoylation[37–39] and interactions with many other proteins. Perhaps not surprisingly, BRCA1 is not only involved in HR but also in many other processes like cell-cycle control and transcriptional regulation[39,40]. Despite its widespread expression and non–cell type–specific functions, mutations in BRCA1 are mainly associated with increased risk of breast and ovarian tumorigenesis. Loss of BRCA1 leads to severe proliferation defects in normal, non-cancerous cells—for instance, leading to lethality during embryonic development. Therefore, it seems likely that there are survival factors that allow BRCA1-deficient tumor cells to expand. In an unbiased genetic screen, we found that loss of 53BP1 rescues clonal outgrowth of *Brca1*-null ES cells. This result confirms the recently described rescue of *Brca1*$^{\Delta11/\Delta11}$ hypomorphic mice by 53BP1 knockout[12]. In addition, it shows that expression of the BRCA1-Δ11 splice variant is not required for rescue of BRCA1 deficiency by 53BP1 loss. This is important, as many human BRCA1-associated cancers are characterized by complete loss of BRCA1 expression. Further characterization indicated that BRCA1 and 53BP1 double-deficient cells are no longer hypersensitive to DNA cross-linking agents and do not spontaneously form DSBs or activate DDR. Suppression of ionizing radiation–induced CHK2 phosphorylation has been previously observed upon RNA interference–mediated 53BP1 depletion in U2OS cells[13] and in *53bp1*$^{-/-}$ MEFs[41]. Here we show that 53BP1 status specifically affects the spontaneous induction of CHK2 phosphorylation when BRCA1 is lost. Our results are consistent with recently reported data on 53BP1-mediated suppression of DNA resection at DSBs and accumulation of single-stranded DNA ends in BRCA1 and 53BP1 double-deficient cells[42]. In cell-free extracts, DNA damage–induced ATM activation and CHK2 phosphorylation are inhibited by 3′ single-stranded DNA overhangs generated during DNA-break processing in S/G2 (ref. 43). The decreased CHK2 phosphorylation that we observed in 53BP1-depleted *Brca1*-null cells could therefore result from decreased ATM signaling due to increased DNA resection or from increased DSB repair. The latter possibility is supported by the restoration of ionizing radiation–induced RAD51 focus formation and the partial restoration of HR in 53BP1-depleted *Brca1*-null cells.

Although our data suggest that a certain level of HR repair can take place in the absence of both BRCA1 and 53BP1, 53BP1-depleted *Brca1*-null cells remain HR defective, as gene-targeting frequencies in these cells are reduced by a factor of 2–10 when compared to wild-type cells. Consistent with this, BRCA1-deficient tumors show excellent responses to therapies exploiting a HR defect, such as platinum drugs[44] or PARP inhibitors[45]. Also, *Brca1*-mutated mouse mammary tumors are highly sensitive to treatment with PARP inhibitors[46] or platinum drugs[47]. Whereas human *BRCA1*-mutated tumors can develop resistance to carboplatin by genetic reversion of the *BRCA1* mutation[48]—stressing the importance of BRCA1 function for HR—mouse mammary tumor models with large deletions in *Brca1* cannot employ this mechanism and remain sensitive to cisplatin or carboplatin, even after multiple rounds of treatment[47]. In contrast, *Brca1*$^{\Delta11/\Delta11}$ mouse mammary tumors, which only express the BRCA1-Δ11 isoform, readily become resistant to cisplatin despite the fact that *Brca1* exon 11 sequences are irreversibly deleted[49]. This feature might be indicative of residual activity of the BRCA1-Δ11 isoform in HR.

At present, it is not clear whether 53BP1 loss contributes to development, therapy response and/or acquired resistance of BRCA1-deficient tumors. To explore this, we examined 53BP1 expression in independent cohorts of breast cancer patients from the US and Finland. These two tumor sets were analyzed by different antibodies and reviewed by independent pathologists using separate criteria, yet both cohorts showed a striking correlation of low 53BP1 expression levels with triple-negative

tumors. Since most *BRCA1*-mutated breast cancers cluster in this subgroup, it was not unexpected to find that these tumors also lacked 53BP1 expression more often than other subsets of breast tumors. However, the often hormone receptor–positive BRCA2-associated tumors were also significantly enriched for 53BP1 aberrations. This may be indicative of a common selection for 53BP1 ablation in both types of HR-deficient breast cancers. This might occur via different routes, given the persistence of DDR activation and growth impairment in 53BP1-depleted BRCA2-deficient cells.

In conclusion, we have shown that 53BP1 loss alleviates the proliferation defect and DNA-damage hypersensitivity of *Brca1*-null cells and leads to partial restoration of HR in these cells. Furthermore, aberrant expression of 53BP1 is more common in BRCA1/2 associated breast cancers, which may hint at a role for 53BP1 loss in these tumors. 53BP1 is also lost in a subset of sporadic triple-negative breast cancers, suggesting a broader role for abnormalities in this pathway in breast tumorigenesis. Our results suggest that loss of 53BP1 may promote survival of BRCA1-deficient tumor cells after DNA damage induced by chemotherapy or irradiation. It is possible that 53BP1 loss may have different effects in BRCA1-deficient tumors versus sporadic triple-negative breast cancers. Regardless, 53BP1 might represent a candidate biomarker for predicting the response of HR-defective tumors to PARP inhibitors or platinum drugs.

METHODS

Methods and any associated references are available in the online version of the paper at http://www.nature.com/nsmb/.

Note: Supplementary information is available on the Nature Structural & Molecular Biology website.

Published online at http://www.nature.com/nsmb/.
Reprints and permissions information is available online at http://npg.nature.com/reprintsandpermissions/.

1. Venkitaraman, A.R. Cancer susceptibility and the functions of BRCA1 and BRCA2. *Cell* **108**, 171–182 (2002).
2. Gudmundsdottir, K. & Ashworth, A. The roles of BRCA1 and BRCA2 and associated proteins in the maintenance of genomic stability. *Oncogene* **25**, 5864–5874 (2006).
3. Boulton, S.J. Cellular functions of the BRCA tumour-suppressor proteins. *Biochem. Soc. Trans.* **34**, 633–645 (2006).
4. Collins, N. *et al.* Consistent loss of the wild type allele in breast cancers from a family linked to the BRCA2 gene on chromosome 13q12–13. *Oncogene* **10**, 1673–1675 (1995).
5. Smith, S.A., Easton, D.F., Evans, D.G. & Ponder, B.A. Allele losses in the region 17q12–21 in familial breast and ovarian cancer involve the wild-type chromosome. *Nat. Genet.* **2**, 128–131 (1992).
6. Johannsson, O.T. *et al.* Tumour biological features of BRCA1-induced breast and ovarian cancer. *Eur. J. Cancer* **33**, 362–371 (1997).
7. Foulkes, W.D. *et al.* Germline BRCA1 mutations and a basal epithelial phenotype in breast cancer. *J. Natl. Cancer Inst.* **95**, 1482–1485 (2003).
8. Sorlie, T. *et al.* Repeated observation of breast tumor subtypes in independent gene expression data sets. *Proc. Natl. Acad. Sci. USA* **100**, 8418–8423 (2003).
9. Turner, N., Tutt, A. & Ashworth, A. Hallmarks of 'BRCAness' in sporadic cancers. *Nat. Rev. Cancer* **4**, 814–819 (2004).
10. Evers, B. & Jonkers, J. Mouse models of BRCA1 and BRCA2 deficiency: past lessons, current understanding and future prospects. *Oncogene* **25**, 5885–5897 (2006).
11. Hakem, R., de la Pompa, J.L., Elia, A., Potter, J. & Mak, T.W. Partial rescue of Brca1 (5–6) early embryonic lethality by p53 or p21 null mutation. *Nat. Genet.* **16**, 298–302 (1997).
12. Cao, L. *et al.* A selective requirement for 53BP1 in the biological response to genomic instability induced by Brca1 deficiency. *Mol. Cell* **35**, 534–541 (2009).
13. Wang, B., Matsuoka, S., Carpenter, P.B. & Elledge, S.J. 53BP1, a mediator of the DNA damage checkpoint. *Science* **298**, 1435–1438 (2002).
14. Morales, J.C. *et al.* 53BP1 and p53 synergize to suppress genomic instability and lymphomagenesis. *Proc. Natl. Acad. Sci. USA* **103**, 3310–3315 (2006).
15. Ward, I.M. *et al.* 53BP1 cooperates with p53 and functions as a haploinsufficient tumor suppressor in mice. *Mol. Cell. Biol.* **25**, 10079–10086 (2005).
16. Xu, X. *et al.* Genetic interactions between tumor suppressors Brca1 and p53 in apoptosis, cell cycle and tumorigenesis. *Nat. Genet.* **28**, 266–271 (2001).
17. Hakem, R. *et al.* The tumor suppressor gene Brca1 is required for embryonic cellular proliferation in the mouse. *Cell* **85**, 1009–1023 (1996).
18. Liu, X. *et al.* Somatic loss of BRCA1 and p53 in mice induces mammary tumors with features of human BRCA1-mutated basal-like breast cancer. *Proc. Natl. Acad. Sci. USA* **104**, 12111–12116 (2007).
19. Hameyer, D. *et al.* Toxicity of ligand-dependent Cre recombinases and generation of a conditional Cre deleter mouse allowing mosaic recombination in peripheral tissues. *Physiol. Genomics* **31**, 32–41 (2007).
20. Wang, W. *et al.* Chromosomal transposition of PiggyBac in mouse embryonic stem cells. *Proc. Natl. Acad. Sci. USA* **105**, 9290–9295 (2008).
21. Bartz, S.R. *et al.* Small interfering RNA screens reveal enhanced cisplatin cytotoxicity in tumor cells having both BRCA network and TP53 disruptions. *Mol. Cell. Biol.* **26**, 9377–9386 (2006).
22. Kastan, M.B. & Bartek, J. Cell-cycle checkpoints and cancer. *Nature* **432**, 316–323 (2004).
23. Taylor, W.R. & Stark, G.R. Regulation of the G2/M transition by p53. *Oncogene* **20**, 1803–1815 (2001).
24. Silver, D.P. & Livingston, D.M. Self-excising retroviral vectors encoding the Cre recombinase overcome Cre-mediated cellular toxicity. *Mol. Cell* **8**, 233–243 (2001).
25. Jonkers, J. *et al.* Synergistic tumor suppressor activity of BRCA2 and p53 in a conditional mouse model for breast cancer. *Nat. Genet.* **29**, 418–425 (2001).
26. Jazayeri, A. *et al.* ATM- and cell cycle-dependent regulation of ATR in response to DNA double-strand breaks. *Nat. Cell Biol.* **8**, 37–45 (2006).
27. Bhattacharyya, A., Ear, U.S., Koller, B.H., Weichselbaum, R.R. & Bishop, D.K. The breast cancer susceptibility gene BRCA1 is required for subnuclear assembly of Rad51 and survival following treatment with the DNA cross-linking agent cisplatin. *J. Biol. Chem.* **275**, 23899–23903 (2000).
28. te Riele, H., Robanus-Maandag, E. & Berns, A. Highly efficient gene targeting in embryonic stem cells through homologous recombination with isogenic DNA constructs. *Proc. Natl. Acad. Sci. USA* **89**, 5128–5132 (1992).
29. te Riele, H., Robanus-Maandag, E., Clarke, A., Hooper, M. & Berns, A. Consecutive inactivation of both alleles of the pim-1 proto-oncogene by homologous recombination in embryonic stem cells. *Nature* **348**, 649–651 (1990).
30. Holstege, H. *et al.* High incidence of protein-truncating TP53 mutations in BRCA1-related breast cancer. *Cancer Res.* **69**, 3625–3633 (2009).
31. Manie, E. *et al.* High frequency of TP53 mutation in BRCA1 and sporadic basal-like carcinomas but not in BRCA1 luminal breast tumors. *Cancer Res.* **69**, 663–671 (2009).

32. Ludwig, T., Chapman, D.L., Papaioannou, V.E. & Efstratiadis, A. Targeted mutations of breast cancer susceptibility gene homologs in mice: lethal phenotypes of Brca1, Brca2, Brca1/Brca2, Brca1/p53, and Brca2/p53 nullizygous embryos. *Genes Dev.* **11**, 1226–1241 (1997).

33. Wang, Y. *et al.* Gene-expression profiles to predict distant metastasis of lymph-node-negative primary breast cancer. *Lancet* **365**, 671–679 (2005).

34. Alexe, G. *et al.* High expression of lymphocyte-associated genes in node-negative HER2+ breast cancers correlates with lower recurrence rates. *Cancer Res.* **67**, 10669–10676 (2007).

35. Richardson, A.L. *et al.* X chromosomal abnormalities in basal-like human breast cancer. *Cancer Cell* **9**, 121–132 (2006).

36. Scully, R. *et al.* Dynamic changes of BRCA1 subnuclear location and phosphorylation state are initiated by DNA damage. *Cell* **90**, 425–435 (1997).

37. Bartek, J. & Hodny, Z. SUMO boosts the DNA damage response barrier against cancer. *Cancer Cell* **17**, 9–11 (2010).

38. Galanty, Y. *et al.* Mammalian SUMO E3-ligases PIAS1 and PIAS4 promote responses to DNA double-strand breaks. *Nature* **462**, 935–939 (2009).

39. Morris, J.R. *et al.* The SUMO modification pathway is involved in the BRCA1 response to genotoxic stress. *Nature* **462**, 886–890 (2009).

40. Deng, C.X. BRCA1: cell cycle checkpoint, genetic instability, DNA damage response and cancer evolution. *Nucleic Acids Res.* **34**, 1416–1426 (2006).

41. Ward, I.M., Minn, K., van Deursen, J. & Chen, J. p53 Binding protein 53BP1 is required for DNA damage responses and tumor suppression in mice. *Mol. Cell. Biol.* **23**, 2556–2563 (2003).

42. Bunting, S.F. *et al.* 53BP1 inhibits homologous recombination in Brca1-deficient cells by blocking resection of DNA breaks. *Cell* **141**, 243–254 (2010).

43. Shiotani, B. & Zou, L. Single-stranded DNA orchestrates an ATM-to-ATR switch at DNA breaks. *Mol. Cell* **33**, 547–558 (2009).

44. Silver, D.P. *et al.* Efficacy of neoadjuvant Cisplatin in triple-negative breast cancer. *J. Clin. Oncol.* **28**, 1145–1153 (2010).

45. Fong, P.C. *et al.* Inhibition of poly(ADP-ribose) polymerase in tumors from BRCA mutation carriers. *N. Engl. J. Med.* **361**, 123–134 (2009).

46. Rottenberg, S. *et al.* High sensitivity of BRCA1-deficient mammary tumors to the PARP inhibitor AZD2281 alone and in combination with platinum drugs. *Proc. Natl. Acad. Sci. USA* **105**, 17079–17084 (2008).

47. Rottenberg, S. *et al.* Selective induction of chemotherapy resistance of mammary tumors in a conditional mouse model for hereditary breast cancer. *Proc. Natl. Acad. Sci. USA* **104**, 12117–12122 (2007).

48. Swisher, E.M. *et al.* Secondary BRCA1 mutations in BRCA1-mutated ovarian carcinomas with platinum resistance. *Cancer Res.* **68**, 2581–2586 (2008).

49. Shafee, N. *et al.* Cancer stem cells contribute to cisplatin resistance in Brca1/p53-mediated mouse mammary tumors. *Cancer Res.* **68**, 3243–3250 (2008).

ONLINE METHODS

$R26^{CreERT2}$ $Brca1^{SCo/\Delta}$ ES cells and mutagenesis screen. Details on the generation of $R26^{CreERT2}$ $Brca1^{SCo/\Delta}$ ES cells and the piggyBac transposon mutagenesis screen are described in **Supplementary Methods**.

MEF isolation and immortalization. Heads and organs of E13.5 embryos were removed, and the remaining tissue was minced, rinsed in PBS and incubated for 30 min in 0.5 ml 0.05% (w/v) trypsin-EDTA (GIBCO) at 37 °C. Cell aggregates were dissociated in DMEM supplemented with 10% (v/v) FBS (GIBCO) and penicillin-streptomycin (GIBCO). Cells were plated on 10-cm dishes and cryopreserved after 2 d as passage 1 MEFs. MEFs were immortalized by infection with TBX2 retrovirus[50].

Retroviral transductions. MEFs were transduced with pRetroSuper retroviruses encoding shRNAs targeting GFP[51], 53BP1 (sh1, 5′-GCTATTGTGGAGATT GTGTTT-3′; sh2, 5′-GCGTAGAAGATATTTCACCTA-3′) or p53 (ref. 52) as described previously[53] (**Supplementary Table 2**). Briefly, HEK 293T packaging cells were transfected with pCL-Eco helper vector together with either pRetroSuper alone or pRetroSuper plus retroviral vector encoding H&R Cre recombinase[24]. The culture medium was replaced 24 h after transfection. Recipient MEFs were plated and then were infected 24 h later with retroviral supernatants. Additional infections were performed after 24 and 32 h. Twenty-four hours after the last infection, cells were washed and grown in medium containing 2–3 mg ml^{-1} puromycin.

Lentiviral transductions. $R26^{CreERT2}$ $Brca1^{SCo/\Delta}$ ES cells were transduced with pLKO-puro shRNA lentiviruses obtained from Mission library clones (Sigma). In addition to the 53BP1 shRNAs mentioned above, we used shRNAs targeting p53 (sh1, 5′-CTACAAGAAGTCACAGCACAT-3′; sh2, 5′-AGAGTATTTCACCCTCAAGAT-3′) and a nontargeting shRNA (SHC202, 5′-CAACAAGATGAAGAGCACCAA-3′) (**Supplementary Table 2**). After selection with 1.8 μg ml^{-1} puromycin, cells were switched by overnight incubation with 0.5 μM 4OHT. Four days after switching, cells were seeded at 1,000 cells cm^{-2} and assayed for clonal growth. Surviving colonies were fixed in formalin and stained with crystal violet.

Cell-cycle analysis. Cells were incubated with BrdU for 1 h, fixed with ethanol and incubated with mouse anti-BrdU (clone BU20A, Dako) and goat anti–mouse FITC conjugated secondary antibodies (DAKO). Cell-cycle distribution was measured by flow cytometry and analyzed using FlowJo software (FlowJo).

Cytotoxicity assays. $R26^{CreERT2}$ $Brca1^{SCo/\Delta}$ ES cells were seeded in triplicate at 1,000 or 3,000 (in the case of switched cells with nontargeting shRNA) cells per well in 96-well plates. One day after seeding, cells were fed with medium containing either cisplatin or mitomycin C. Five days later, cell viability was assayed in an Envision plate reader (Perkin Elmer) using resazurin (cell titer blue, Promega).

MEF proliferation assays. Primary MEFs were seeded at 5,000 cells per well in 96-well plates. Cell number was determined after 24, 48, 72 and 96 h by incubating cells with 10 micrograms ml^{-1} resazurin. After 2 h, fluorescence was measured at 590 nm using a microtiter plate reader (2103 multilabel reader, Perkin Elmer).

Analysis of chromosomal aberrations. Exponentially growing MEFs were either collected and processed for immunoblotting as described below or processed for metaphase spreads preparation. For this, cells were treated with 0.1 μg ml^{-1} colcemid for 4 h or 16 h, trypsinized, swollen in hypotonic buffer (10 mM Tris-HCl, pH7.5, 10 mM NaCl, 5 mM MgCl$_2$) at 37 °C for 5 min and fixed in 3:1 methanol:glacial acetid acid.

Immunoblotting. Cells were harvested by trypsinization, washed twice with cold HBSS, resuspended in SDS-PAGE loading buffer and sonicated. Equal amounts of protein were analyzed by gel electrophoresis followed by western blotting.

NuPAGE-Novex 10% (w/v) bis-Tris gels or Tris-acetate 3–8% (w/v) (Invitrogen) were run according to the manufacturer's instructions.

Immunofluorescence. ES cells were grown on coverslips, γ-irradiated with 10 Gy and fixed 6 h later using 2% (w/v) paraformaldehyde in PBS. Fixed cells were incubated with antibody in PBS containing 0.5% (w/v) BSA and 0.15% (w/v) glycine, mounted using Vectashield with 4,6-diamidino-2-phenylindole (DAPI) (Vector Laboratories) and imaged with a Hamamatsu ORCA AG CCD camera on a Zeiss Axio Observer Z1 system. For quantification of RAD51 foci, images were converted into 8-bit gray-scale pictures using Image J software (ImageJ, US National Institutes of Health), and the fluorescence-intensity threshold was set based on a black-and-white intensity scale from 140 to 255. For each sample, the number of foci was counted in at least 20 individual nuclei.

MEFs were grown on coverslips and γ-irradiated with 10 Gy. Cells were allowed to recover for the indicated times, washed in PBS and swollen in hypotonic solution (85.5 mM NaCl, 5 mM MgCl$_2$, adjusted to pH 7.0) for 5 min. Cells were fixed with 4% paraformaldehyde (10-min at room temperature), permeabilized by adding 0.03% (w/v) SDS to the fixative and immunostained as described[54]. Dried coverslips were mounted on microscope slides using the ProLong Antifade kit (Invitrogen) supplemented with 1 mg ml^{-1} DAPI, and viewed with a Leica DMI6000B fluorescence microscope. Images were acquired with a Leica DFC350 FX R2 digital camera using LAS-AF software (Leica). Image brightness and contrast were adjusted using Photoshop CS3 (Adobe). To quantify RAD51 foci, we determined the frequency of nuclei with more than 10 RAD51 foci. At least 50 nuclei were analyzed for each sample.

Antibodies. Antibodies used for immunoblotting of ES cells were mouse monoclonal anti–mouse BRCA1 (GH118), affinity-purified rabbit polyclonal anti–mouse BRCA1 against peptide 452–469, 53BP1 (ab21083, Abcam) and p53 (IMX25, Monosan). Immunocytochemical staining of ES cells was performed using human RAD51 (ref. 54) and goat anti–rabbit Alexa 588 secondary antibody (Molecular Probes).

Antibodies used for immunobloting of MEFs were human RAD51 (ref. 54), SMC1 (BL308, Bethyl), 53BP1 (NB100-304, Novus), p53 (1C12, Cell Signaling), Chk2 (clone 7, Millipore) and α-tubulin[54] (CRUK Monoclonal Antibody Service). Antibodies for imunofluorescence staining of MEFs were mouse monoclonal anti–phospho histone H2AX-Ser139 (Upstate Biotechnology) and RAD51 (H-92, Santa Cruz biotechnologies).

Gene-targeting assays. $R26^{CreERT2}$ $Brca1^{SCo/\Delta}$ ES cells were electroporated with linearized Rb-neo[28] or $Pim1$-neo[29] targeting constructs. After drug selection with 200 μg ml^{-1} G418, colonies were picked, expanded and lysed in direct lysis reagent (Viagen) containing 100 μg ml^{-1} proteinase K. Following heat inactivation of proteinase K, genomic DNA was used for PCR analysis or digested with appropriate restriction enzymes and analyzed by Southern blotting as described[28,29].

Analysis of 53BP1 expression in human breast cancers. Details on analysis of 53BP1 expression in human breast cancers using tissue microarrays from the Yale and Helsinki cohorts or gene expression array datasets from previous reports[33,35] are described in **Supplementary Methods**.

50. Jacobs, J.J. *et al.* Senescence bypass screen identifies TBX2, which represses Cdkn2a (p19(ARF)) and is amplified in a subset of human breast cancers. *Nat. Genet.* **26**, 291–299 (2000).
51. Tarsounas, M. *et al.* Telomere maintenance requires the RAD51D recombination/repair protein. *Cell* **117**, 337–347 (2004).
52. Dirac, A.M. & Bernards, R. Reversal of senescence in mouse fibroblasts through lentiviral suppression of p53. *J. Biol. Chem.* **278**, 11731–11734 (2003).
53. Palmero, I. & Serrano, M. Induction of senescence by oncogenic Ras. *Methods Enzymol.* **333**, 247–256 (2001).
54. Tarsounas, M., Davies, D. & West, S.C. BRCA2-dependent and independent formation of RAD51 nuclear foci. *Oncogene* **22**, 1115–1123 (2003).